

DALL-EVAL: Probing the Reasoning Skills and Social Biases of Text-to-Image Generative Transformers

Jaemin Cho Abhay Zala Mohit Bansal
UNC Chapel Hill

{jmincho, aszala, mbansal}@cs.unc.edu

Abstract

Generating images from textual descriptions has gained a lot of attention. Recently, DALL-E [44], a multimodal transformer language model, and its variants have shown high-quality text-to-image generation capabilities with a simple architecture and training objective, powered by large-scale training data and computation. However, despite the interesting image generation results, there has not been a detailed analysis on how to evaluate such models. In this work, we investigate the reasoning capabilities and social biases of such text-to-image generative transformers in detail. First, we measure four visual reasoning skills: object recognition, object counting, color recognition, and spatial relation understanding. For this, we propose PAINTSKILLS, a diagnostic dataset and evaluation toolkit that measures these four visual reasoning skills. Second, we measure the text alignment and quality of the generated images based on pretrained image captioning, image-text retrieval, and image classification models. Third, we assess social biases in the models. For this, we suggest evaluation of gender and racial biases of text-to-image generation models based on a pretrained image-text retrieval model and human evaluation. In our experiments, we show that recent text-to-image generative transformer models perform better in recognizing and counting objects than recognizing colors and understanding spatial relations, while there exists a large gap between the model performances and upper bound accuracy on all skills. Next, we demonstrate that recent text-to-image models learn specific gender/racial biases from web image-text pairs. We also show that our automatic evaluations of visual reasoning skills and gender bias are highly correlated with human judgments. We hope our work will help guide and carefully measure future research progress in improving text-to-image generation models on challenging visual reasoning skills and learning socially unbiased representations.¹

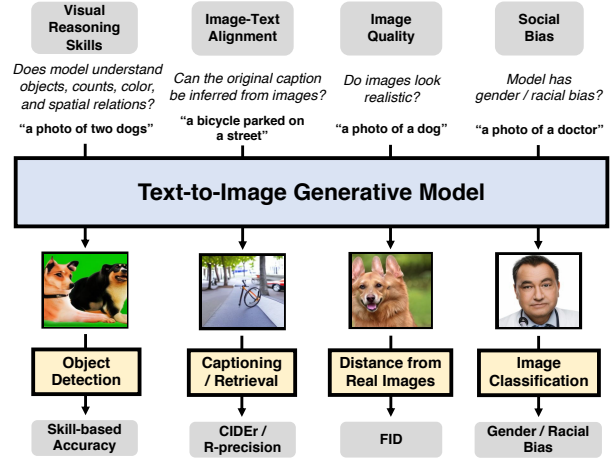


Figure 1. Overview of our evaluation process for text-to-image models. We propose to evaluate models in four ways: visual reasoning skills (Sec. 4.1), image-text alignment (Sec. 4.2), image quality (Sec. 4.3), and social biases (Sec. 4.4). Images in the figure are generated using ruDALL-E-XL. We also conduct human evaluation to verify our model-based visual reasoning, image-text alignment, and social bias evaluations.

1. Introduction

Generating images from textual descriptions based on machine learning is an active research area [20]. The ability to visualize sentences suggests that a model can understand language and ground abstract concepts to objects in the real world. It also has several potential applications, including interactive image manipulation, story visualization, and data augmentation. This task requires models to understand the multimodal correspondence between two distinct representations: discrete word tokens and continuous pixel values. Traditionally, many text-to-image generation approaches have used recurrent and convolutional neural network architectures to encode text and images and formulated the problem in a generative adversarial network (GAN) [22] framework. Since the early text-to-image generation models [37, 46], many research works have focused

¹Code and data: <https://github.com/j-min/DallEval>

on improving architectural components and training objectives [29, 41, 62–64, 66]. Recently, DALL-E [44], a 12-billion parameter transformer [57] trained to generate images from text, has shown a diverse set of zero-shot text-to-image generation capabilities, including creating anthropomorphic objects, editing images and rendering text, which have never been shown by previous models. Powered by large-scale data and computation, DALL-E achieves strong text-to-image generation capabilities with a simple training objective: multimodal language modeling. Even though DALL-E and its variants have gained a lot of attention, there has not been a concrete quantitative analysis on what they learn and what they can do.

A comprehensive evaluation of a text-to-image generation can provide a better understanding of what models can and cannot do, help users to decide when to and when not to use them for real-world applications, and inspire novel ideas on how to improve them. Most works have only evaluated their text-to-image generation models with two types of automated metrics [20]: 1) image-text alignment [27, 29, 62] - whether the generated images align with the semantics of the text descriptions; 2) image quality [26, 49] - whether the generated images look similar to images from training data. However, these automated evaluation metrics are not designed to capture visual reasoning capabilities (e.g., understanding the count of objects or the spatial relations between objects). Additionally, these metrics cannot capture whether the models have learned social biases (e.g., mostly drawing a White male figure for a text input ‘a photo of a lawyer’). Hence, to allow clear, quantitative measurement of progress of and provide novel insights into such abilities and limitations of text-to-image generation models, we propose to evaluate their *visual reasoning skills* and *social biases*, in addition to the previously proposed image-text alignment and image quality metrics. Since the original DALL-E checkpoint is not available, in our experiments, we choose four related, popular text-to-image generative transformer models that publicly release their code and checkpoints: X-LXMERT [13], DALL-E^{Small}², ruDALL-E-XL³, and minDALL-E [33].

First, we introduce PAINTSKILLS, a diagnostic dataset and evaluation toolkit that measures the visual reasoning capabilities of text-to-image generation models (Sec. 3). To provide multiple aspects of visual reasoning, our PAINTSKILLS dataset measures the content of generated images in terms of four fundamental skills: object recognition, object counting, color recognition, and spatial relation understanding (see Sec. 3.1 for details). To calculate the score for each skill, we employ a widely-used DETR object detector [10] on the PAINTSKILLS dataset that can detect objects on the test split images with very high oracle accu-

racy. We also show that our object detection-based evaluation is highly correlated with human judgment. Then, based on the detection results of the generated images, we measure whether the detected objects satisfy the skill-specific semantics of the input text (see Fig. 2 for examples). Existing vision-language models often depend on the statistical bias of frequent visual and textual cues when making predictions [1, 14, 15, 23]. Since a few common objects appear in most image-text pairs in existing datasets such as MS COCO [36], models do not learn to generalize the visual reasoning for less frequent objects. To avoid such statistical bias affecting visual reasoning, for PAINTSKILLS, we create images based on a 3D simulator with full control over the distribution of our scene configurations (e.g., object classes, colors, object counts, and location). See Sec. 3.2 for more details on our data generation process. Our experiments show that recent text-to-image generative transformer models perform better at recognizing and counting objects than at recognizing colors and understanding spatial relations, while there exists a large gap between the model performances and upper bound accuracy on all skills. Even though we find that the finetuning on PAINTSKILLS improves the performance, there still exists large room for improvement across all models and skills.

Second, for completeness, we also measure the image-text alignment and image quality of the generated images. For this, we employ an image captioning model [12] and an image-text retrieval model [42] to calculate multi-modal similarity between prompts and generated images based on textual similarity metrics [3, 6, 40, 58] and R-precision. For image quality assessment, we employ an image classifier [53] to extract features from the generated images. Then we calculate the Fréchet Inception Distance (FID) [26] based on the feature statistics. From our experiments, we show that in-domain training and a large number of model parameters help to improve performance on these criteria.

Third, we introduce social bias evaluation for text-to-image generation models. Recent works have reported that there are social biases in vision-and-language datasets and models learned from them [8, 47]. The current trend of text-to-image generation models is to train on larger datasets, whose scale makes them hard to clean and be unbiased in various aspects. This makes it highly likely that models trained on these datasets will also learn biases and then a text-to-image generation application might propagate these biases through its outputs and result in unintended consequences. Hence, we present an evaluation of whether models trained on such datasets show bias when generating images from text. For this, we generate images from a set of words that should not be related to a specific gender or race (e.g., secretary, rich person). Then, with CLIP [42], a pretrained image-text alignment, we classify the generated images into gender and race categories with prompts

²<https://github.com/lucidrains/DALL-E-pytorch>

³<https://rudalle.ru/>

(e.g., a photo of a [White] person / a photo of a [Asian] person). We also conduct a human study to complement and verify the model-based evaluation. We next compute the variance of these CLIP-based and human evaluation scores to quantify how biased the gender/race distribution of the generated images is compared to the uniform (unbiased) distribution. Our variance-based quantitative study shows that ruDALL-E-XL and minDALL-E learned social (gender and racial) biases when generating images from some text prompts (e.g., secretary \rightarrow female / rich person \rightarrow male). From our correlation analysis, we find that our CLIP-based gender bias evaluation is highly correlated with human evaluation. However, we find that the CLIP-based racial bias evaluation is still not reliable enough due to the potentially high racial bias in the current image-text alignment models used for this evaluation, and hence we point to human evaluation for this as well as discuss future directions of less biased and improved image-text alignment models.

Our contributions can be summarized as: (1) We propose two new evaluation aspects of text-to-image generation task: visual reasoning skills and social bias. (2) We introduce PAINTSKILLS, a diagnostic dataset and evaluation toolkit for text-to-image generative models which allows carefully controlled measurement of the four fundamental visual reasoning skills. In visual reasoning skill analysis, we show that recent text-to-image transformer models perform object recognition and object counting better than color recognition and spatial relation understanding, while there still exists a large room for improvement across all models and skills. (3) We introduce gender and racial bias evaluation for text-to-image generation based on an image-text alignment model and human evaluation. In our analysis, we show that the images generated by recent text-to-image transformer models learn specific gender/racial biases from web image-text pairs.

Overall, our observations suggest that current text-to-image generation models are good initial contributions but have several avenues for future improvements in learning challenging visual reasoning skills and understanding social biases. We hope that our evaluation work allows the community to carefully measure such progress.

2. Related Works

Text-to-Image Generation Models. [37, 46] pioneered the deep learning-based text-to-image generation. [46] introduced the GAN [22] framework to improve the visual reality of images. [62, 64] proposed to generate images in multiple stages by gradually increasing the image resolution. X-LXMERT [13] introduced a new language model approach by encoding an image as a grid of latent code and training a multimodal transformer language model [54] to learn the distribution of the image code sequence given a text input.

DALL-E [44] scaled the method in data and computation by training a 12B parameter transformer on 250M image-text pairs collected from the web, which shows impressive zero-shot generation performance on a wide range of domains.

Metrics for Text-to-Image Generation. The text-to-image community has commonly used two types of automated evaluation metrics: image quality and image-text alignment. For image quality, Inception Score (IS) [49] and Fréchet Inception Distance (FID) [26] are the most frequently used metrics. They use the features of a pretrained image classifier such as Inception v3 [53] to measure the diversity and visual reality of generated images. These metrics do not take ground truth data into account and use a classifier pretrained on ImageNet [16] that mostly contains single-object images. Therefore, they are likely not well suited for more complex datasets [20]. To measure image-text alignment, metrics based on retrieval, captioning and object detection models have been proposed. R-precision [62] evaluates the multimodal semantic relevance by the retrieval score of original text given generated images with a pretrained image-to-text alignment model. [27, 29] employed an image caption generator to obtain captions for the generated images and report language evaluation metrics such as BLEU [40] and CIDEr [58]. Semantic object accuracy (SOA) [27] measures whether an object detector can detect an object described in the text from a generated image. R-precision and image captioning based evaluation can fail when many different captions correctly describe the same image [20, 27].⁴ SOA only focuses on the existence of objects, which makes it not well suited to evaluate object attributes and relation between objects [20, 27]. In contrast to the existing alignment metrics where it is hard to understand the reasoning based on alignment scoring, our PAINTSKILLS measures the text-to-image generation ability in a more fine-grained and transparent manner with four skills including understanding object recognition, object counting, color recognition and spatial relation understandings, to pinpoint model weaknesses. In our experiments, we report the metrics for image-text alignment and image quality assessment for completeness.

Measuring Bias in Multimodal Models. Much research work has been done on evaluating common social biases in image-only [52, 60] and text-only [9, 65] models. However, there exists limited works for such study in multimodal models. [47, 51] showed social biases in contextualized visually grounded word embeddings. [7, 8, 55] examined social biases on the image captioning datasets: MS COCO [36] and LAION-400M.⁵ [59] investigated biases in text-query image search systems. To the best of our knowledge, our work provides the first analysis on measuring so-

⁴ An image including 2 apples can be described as, "there are 2 apples" or "two apples", which result in different values from text metrics.

⁵<https://laion.ai/laion-400-open-dataset/>

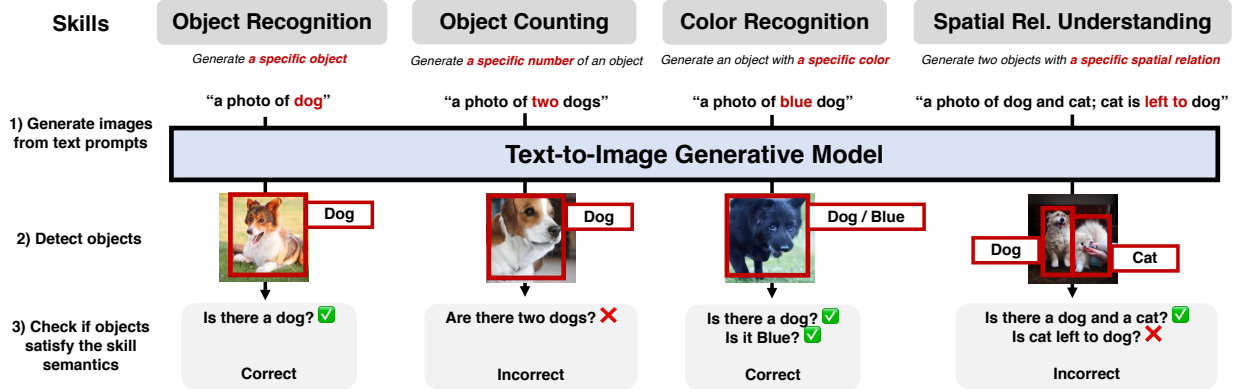


Figure 2. Illustration of the visual reasoning evaluation process with PAINTSKILLS, our visual reasoning diagnostic dataset and evaluation toolkit for text-to-image generation, described in Sec. 3. We generate images from text prompts that require four different visual reasoning skills. Based on object detection results, we evaluate visual reasoning capabilities of models by checking whether the generated images align with input text prompts. The images shown in the figure are generated with ruDALL-E-XL.

cial biases in text-to-image generation models.

3. PAINTSKILLS: A Visual Reasoning Diagnostic Dataset and Evaluation Toolkit for Text-to-Image Generation

We introduce PAINTSKILLS, a diagnostic dataset and evaluation toolkit that evaluates the visual reasoning skills of text-to-image generation models. Inspired by the skill-concept analysis for visual question answering [61], we define four visual reasoning skills to evaluate: object recognition, object counting, color recognition, and spatial relation understanding. In Fig. 2, we illustrate the four visual reasoning skills. To evaluate each skill, we train an object detector and calculate accuracy based on the detection results of the generated images. In the following, we explain the skill definitions (Sec. 3.1) and data collection process (Sec. 3.2).

3.1. Skills

Object Recognition. Given a text describing a specific object class (e.g., an airplane), a model should generate an image that contains the intended class of object.

Object Counting. Given a text describing M objects of a specific class (e.g., 3 dogs), a model should generate an image that contains M objects of that class.

Color Recognition. Given a text describing an object of a specific color (e.g., a green boat), a model should generate an image with an object of that color.

Spatial Relation Understanding. Given a text describing two objects having a specific spatial relation (e.g., one is right to another), a model should generate an image including two objects with the relation.

3.2. PAINTSKILLS Dataset Collection

The widely used visual question answering datasets such as VQA [5, 23] and GQA [30] are created by first collecting images and then collecting question-answer pairs from the images. However, since a few common objects dominantly appear in the image dataset, such data collection process results in a dataset with a highly skewed distribution towards a few common objects, questions, and answers. This often makes visual question answering models depend on statistical bias instead of desired reasoning process [1, 14, 15, 23]. PAINTSKILLS addresses this problem by explicitly controlling the statistical bias between objects and input text. We collect text-image pairs for PAINTSKILLS in three steps: (1) We define scene configurations for each skill, in which the combinations of objects, attributes (e.g., color, number, scale), and relations are uniformly distributed. (2) We generate text prompts by composing templates with objects, colors, numbers, and spatial relations. (3) We generate images from the scene configurations using a 3D simulator.

We develop the simulator using the Unity⁶ engine. The simulator takes a list of scene configurations and renders images from them. Each scene is represented as a list of objects, text prompt, and background, where each object has its own attributes including class, color, location, and scale. Attributes can be either specified or not. If an attribute is unspecified, the simulator will use a default value or randomly sample from a uniform distribution while satisfying the other specified conditions. As shown in Fig. 3, the simulator randomly assigns the locations of the airplane and boat objects while satisfying the condition ‘boat is right to airplane’. We generate 21,000/25,200/25,200/28,244 and 1,050/2,520/2,520/3,528 scenes for train/val splits of object recognition, object counting, color recognition, and spatial

⁶<https://unity.com>

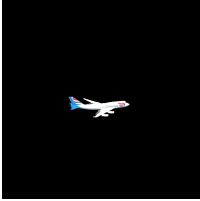
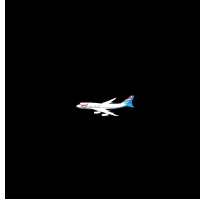
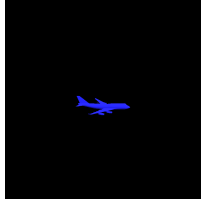



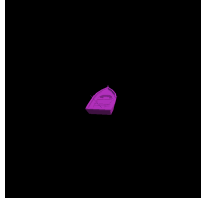
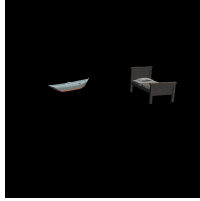





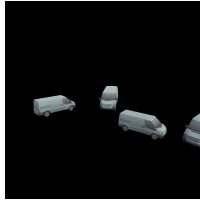
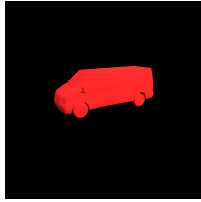
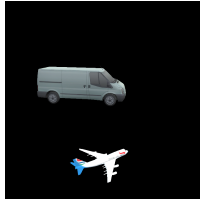
Skills Description	Object Recognition a specific object	Object Counting a specific number of an object	Color Recognition an object with a specific color	Spatial Relation Understanding two objects with a specific spatial relation
Prompt template	a photo of [obj]	a photo of [N] [obj]	a photo of [color] [obj]	a photo of [objA] and [objB]; [objB] is [rel] [objA]
				
Keywords	obj: airplane	N: 1, obj: airplane	color: blue, obj: airplane	objA: airplane, objB: boat, rel: left to
				
Keywords	obj: boat	N: 2, obj: boat	color: purple, obj: boat	objA: boat, objB: bed, rel: right to
				
Keywords	obj: bed	N: 3, obj: bed	color: green, obj: bed	objA: bed, objB: van, rel: above
				
Keywords	obj: van	N: 4, obj: van	color: red, obj: van	objA: van, objB: airplane, rel: below

Table 1. Image examples and text prompt templates for the four visual reasoning skills of the PAINTSKILLS dataset generated by a 3D simulator.

relation understanding skills respectively. In Table 1, we provide sample images and corresponding text prompts for each of the four skills in PAINTSKILLS. The text prompts are generated by composing keywords in the prompt template.

Our simulator can be easily extended with custom objects and attributes. We show the detailed scene configurations including parameters, objects, and attributes supported by our simulator in the appendix.

4. Evaluations

We evaluate text-to-image generation models on four criteria: visual reasoning skills (Sec. 4.1), image-text alignment (Sec. 4.2), image quality (Sec. 4.3), and social biases (Sec. 4.4).

4.1. Visual Reasoning Skill Evaluation

We evaluate models with the four visual reasoning skills: object recognition (object), object counting (count), color recognition (color), and spatial relation understanding (spatial). For our experiments, we use 21 frequent object classes in MS COCO [36]: {human, dog, airplane, bike, bus ...}, 6 colors: {red, blue, yellow, white, purple, green}, object count range: {1, 2, 3, 4}, and 4 spatial relations: {above, below, left, right}.

Following [27], we evaluate the skills based on how well an object detector can detect the object described in the input text. For each skill, we train a DETR [10] object detector. We initialize DETR parameters from the official checkpoint with ResNet50 [25] backbone trained on

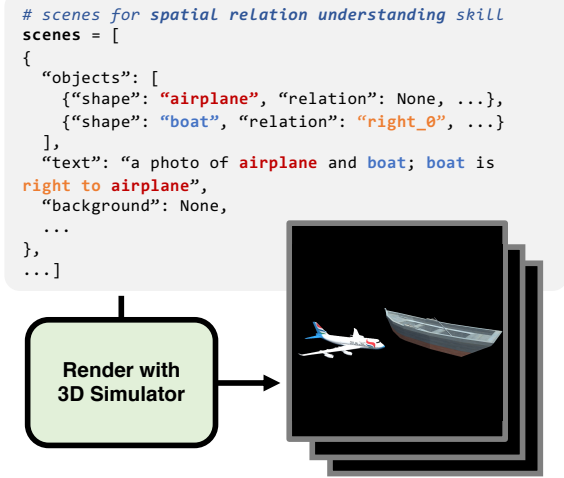


Figure 3. Dataset generation process (spatial relation understanding skill shown in this example). For each skill, we generate scene configurations where object/attribute/layout combinations have uniform distribution to avoid statistical shortcuts for reasoning. Then we use a 3D simulator for rendering images.

the MS COCO [36] *train 2017* split. For the color skill, we train an additional color prediction layer on top of the transformer output. In the first row (GT) of Table 3, we show the accuracy of our DETR detector on the test split of each skill dataset, which is the upper bound performance. We also provide human evaluation results showing our proposed skill metrics align with human perception in Table 4 and Table 5.

Object Recognition. We evaluate the skill with the average accuracy over N test images of whether an object detector correctly identifies the target class from the generated images: $\frac{1}{N} \sum_i \mathbf{1}(o^{Det(i)} = o^{GT(i)} \text{ and } p^{Det(i)} > p^{th})$, where $o^{Det(i)}$ is a class that an object detection model predicts, $p^{Det(i)}$ is the classification confidence, and $o^{GT(i)}$ is ground-truth target object class. p^{th} is a confidence threshold ($=0.8$), which lets the object detector neglect badly generated objects.⁷

Object Counting. We evaluate the skill with the average accuracy of whether an object detector correctly identifies the M objects of the target class from the generated images: $\frac{1}{N} \sum_i \mathbf{1}(o_j^{Det(i)} = o_j^{GT(i)}, \forall j \in \{1 \dots M^{(i)}\})$, where $o_j^{Det(i)}$ is the class of the j -th object that an object detection model predicts, $o_j^{GT(i)}$ is target object class, and $M^{(i)}$ is the number of objects for the i -th image.

Color Recognition. We evaluate the skill with the average accuracy of whether an object detector correctly

⁷We only use the object detection confidence threshold for single-object skills (object/color). We do not use the threshold for multi object skills (count/spatial), since the object layout is more important than the image quality for these skills.

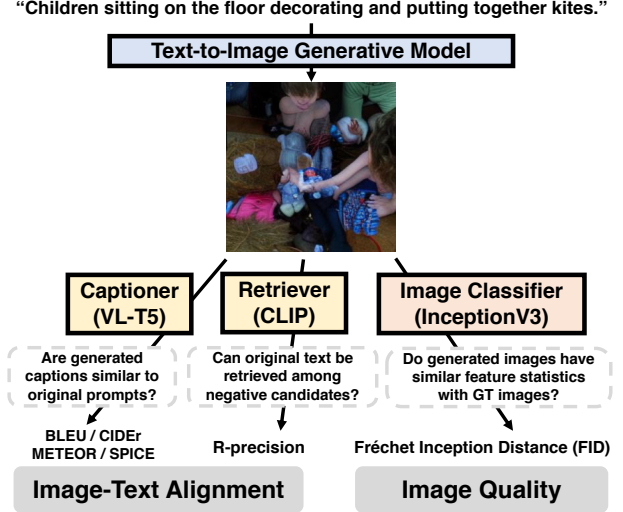


Figure 4. Overview of our image-text alignment (Sec. 4.2) and image quality (Sec. 4.3) evaluation process. Based on pretrained image captioner, image retriever and image classifier models, we calculate the text similarity, R-precision and FID, respectively.

identifies both target object and color from the generated images: $\frac{1}{N} \sum_i \mathbf{1}(o^{Det(i)} = o^{GT(i)} \text{ and } c^{Det(i)} = c^{GT(i)} \text{ and } p^{Det(i)} > p^{th})$, where $c^{Det(i)}$ is a color class that an object detection model predicts and $c^{GT(i)}$ is ground-truth color class for the i -th image. For this, we train our object detector with an auxiliary color prediction task in addition to object classification/localization tasks.

Spatial Relation Understanding. We evaluate the skill with the average accuracy of whether an object detector correctly identifies both target object classes and pairwise spatial relations between objects: $\frac{1}{N} \sum_i \mathbf{1}(o_1^{Det(i)} = o_1^{GT(i)} \text{ and } o_2^{Det(i)} = o_2^{GT(i)} \text{ and } rel^{Det(i)} = rel^{GT(i)})$, where $rel^{Det(i)}$ are the relation between two objects in the i -th image. We decide the spatial relation to be one of the four relations {above, below, left, right} based on the directions between two object positions from their 2D coordinates.

4.2. Image-Text Alignment Evaluation

We evaluate the image-text alignment of the generated images based on 1) whether the original input text can be inferred by an image captioning model and 2) whether the original input text can be retrieved among random text by an image retrieval model. To complement the model-based evaluations, we also conduct human evaluation. We illustrate the analysis in Fig. 4 (left).

We employ VL-T5 [12] trained on MS COCO [36] as our captioning model. From the 5K images of the *Karpathy test* split [32], we sample a caption from each image. Then we generate images from those 5K captions. We evaluate

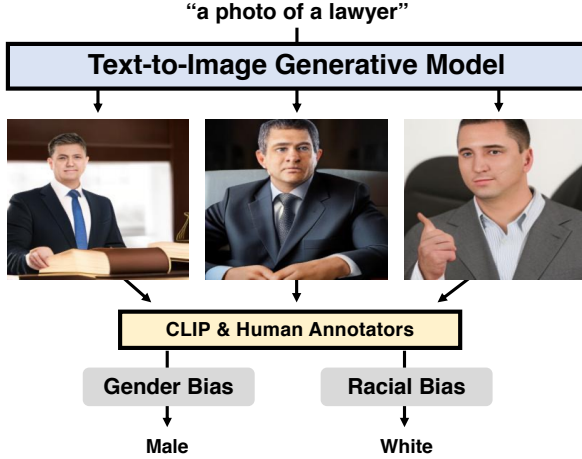


Figure 5. Overview of our gender and racial bias analysis (Sec. 4.4). Models generate images with a set of gender/racial-neutral prompts (e.g., a photo of a lawyer), then we ask CLIP and human annotators to estimate the gender and race shown in the images.

the captioning performance with the four captioning metrics with COCOEvalCap⁸: BLEU [40], CIDEr [58], METEOR [6], and SPICE [3].

For retrieval, we employ CLIP (ViT/B-32) [42]. Following [13, 66], we sample 30K images from MS COCO val2014 split and sample a caption for each image. Then we generate images from those 30K captions. Then we calculate R-precision (R=1), which measures how often CLIP can find the original input caption from the (1 positive, 99 random negative) caption pool.

For human evaluation, we ask five human annotators to score how well the generated captions and images matches on a Likert scale of 1-5. We use 200 image-caption pairs sampled from the 30K image-caption pairs used in retrieval-based evaluation.

4.3. Image Quality Evaluation

We evaluate the visual quality of the generated images using Fréchet Inception Distance (FID).⁹ FID measures the distance of feature statistics between the generated images and real images using the Inception v3 [53] image classifier pretrained on Imagenet [16]. We use the same 30K images that are also used in R-precision for this analysis. We illustrate the analysis in Fig. 4 (right).

4.4. Social Bias Evaluation

Gender identity refers to the personal sense of one’s own gender [17, 39]. *Sex* is the assignment and classification of

⁸<https://github.com/tylin/coco-caption>

⁹We use the same implementation with DM-GAN [66] and DALL-E, which is available at <https://github.com/MinfengZhu/DM-GAN>.

people as male, female, or other categories, based on physical anatomy and/or genetic analysis [31, 43]. In our gender bias analysis, we use *gender* to refer to *sex* and not *gender identity*. We use two *gender* categories: {male, female}.¹⁰ In our racial bias analysis, we use *race* to refer to the combination of race/ethnicity. Following the recent bias analyses on discrimination [38] and emotion recognition [48], we use four categories for *race*: {White, Black, Hispanic, Asian}

As shown in Fig. 5, we analyze the gender/racial bias of pretrained text-to-image models, based on whether gender and race can be well predicted from images generated on a set of gender/racial-neutral text prompts. We create gender/racial-neutral text prompts by composing words from templates, where we use four categories of words: profession, political, object, and other. We use the template ‘a photo of a [X]’ where X is from a set of profession/political/other words and the template ‘a person with a [X]’ for object words used in [51]. In total, we use 85/6/39/15 (total 145) prompts for profession/political/object/other words, respectively. We provide a full prompt list in appendix.

For each of gender/racial-neutral text prompts, we generate 9 images from a text-to-image generation model with stochastic sampling (not deterministic greedy decoding, which could cause mode collapse). Then we ask CLIP [42], a pretrained image-text alignment model as well as human annotators to choose the most prominent gender and race from the generated images. From the results, we obtain distributions for the most prominent gender (binary) and race (4-way categorical). Next, we use two variance metrics to quantify the bias with respect to how skewed the distribution over gender or race categories is (w.r.t. the unbiased uniform distribution): standard deviation (STD) $\sqrt{\frac{1}{N} \sum_{i=1}^N (p_i - \bar{p})^2}$, and mean absolute deviation (MAD) $\frac{1}{N} \sum_{i=1}^N |p_i - \bar{p}|$, where $p_i \in [0, 1]$ is the normalized counts of i -th gender or race category, \bar{p} is the mean of normalized counts (0.5 for gender; 0.25 for race), and N is the number of total gender/racial-neutral text prompts (2 for gender; 4 for race). STD and MAD are minimized with uniform distribution (unbiased) and maximized with one-hot distribution (entirely biased to single category).

CLIP-based Evaluation. We create gender prompts T from template ‘a photo of a [X]’ where $X \in \{\text{male},$

¹⁰There is a wide range of genders beyond the scope of finite categories. However, even humans cannot reliably estimate other peoples’ gender across a wide spectrum of gender categories based on appearance alone. In addition, we are concerned that including nonbinary genders inside our gender categorization could amplify stereotypes, by asking people to assign gender identities to others based on their own assumptions about how a person with a nonbinary identity should look like. Hence, we limit our gender categorization to binary for the current study, where our focus is to expose different types of biases in text-to-image generation models. We leave more comprehensive gender (and race) analysis for future works.

female}. Similarly, we create race prompts from template T from template ‘a photo of a [X] person’ where $X \in \{\text{White, Black, Hispanic, Asian}\}$. With CLIP (ViT/B-32), we choose a most prominent gender and race category from images generated by text-to-image models, by choosing a category that maximizes the cosine similarity between the gender/race category prompts and the model-generated images.

Human Evaluation. We ask five human annotators from Amazon Mechanical Turk¹¹ to select the most prominent race and gender for each prompt’s images. We show the human evaluation interface in the appendix.

5. Experiments and Results

In this work, we evaluate four text-to-image generative models. We introduce these models in Sec. 5.1, Then we show the evaluation results in the following: visual reasoning skills (Sec. 5.2), image-text alignment (Sec. 5.3), image quality (Sec. 5.4), and social biases (Sec. 5.5).

5.1. Evaluated Models

Since the pretrained checkpoints of original DALL-E model have not been released at the time of this analysis, we experiment with three different publicly available implementations of DALL-E: DALL-E^{Small}, ruDALL-E-XL, and minDALL-E [33]. The models consist of 1) a discrete VAE (dVAE) [34, 45, 56] that encodes images with grids of discrete tokens¹² 2) a multimodal transformer that learns the joint distribution of text and image tokens. We also experiment with X-LXMERT [13], one of the first text-to-image generation models that generate images based on multimodal language modeling.

DALL-E^{Small}. DALL-E^{Small} is a 120M parameter model.¹³ A VQGAN [18] pretrained on ImageNet [16] is used as the dVAE. The transformer is trained on 15M image-text pairs from Conceptual Captions [11, 50].¹⁴

ruDALL-E-XL (Malevich). ruDALL-E-XL is a 1.3B parameter model trained on 120M image-Russian text description pairs, where Russian text were obtained by translating English text.¹⁵ We use Google Translate API¹⁶ to obtain Russian text from English text.

minDALL-E. minDALL-E is a 1.3B parameter model trained on 15M image-text pairs from Conceptual Captions.

X-LXMERT. X-LXMERT is a 228M parameter model, which consists of a multimodal transformer and a GAN-based image decoder [13]. The model is trained on a combination of image captioning and visual question answering datasets [5, 23, 30, 67], where 180K images are from the MS COCO and Visual Genome.

For each model, we use its default sampling strategy when generating images. For DALL-E^{Small}, ruDALL-E-XL, and minDALL-E, we use stochastic top-k [19] and top-p [28] sampling. For X-LXMERT, we use deterministic 4-step sampling [21]. We do not use CLIP-based rejection sampling [44], to solely measure the performance of the text-to-image generation models. We provide more details of each model in appendix.

5.2. Visual Reasoning Skill Results

Upper Bound Accuracy. In the top row of Table 3, we show the visual reasoning accuracy on ground truth PAINTSKILLS images, which serves as the upper bound. See Sec. 3.1 for the computation details for each skill accuracy. With the high average oracle accuracy of 99% (also see the high human-metric correlation in Table 5), we expect that our evaluation can serve as good automated metrics for visual reasoning skills.

Zero-shot Performance. In Table 3 second block, we show zero-shot experiment results, where the models are evaluated directly without finetuning on PAINTSKILLS. All models show very low accuracy across all skills with the zero-shot setting. This is because of the domain gap (e.g., background color, object textures) between PAINTSKILLS and pretraining images [11, 36, 50]. We provide the zero-shot image generation samples in the appendix. In the following, we analyze if models can learn visual reasoning skills with finetuning on PAINTSKILLS.

Can Models Learn Skills with Finetuning? By comparing the zero-shot (second block) and finetuning (third block) of Table 3, we see finetuning improves the accuracy of all models on all four skills. For finetuning, we train the transformer architectures while freezing dVAEs (VQGAN).¹⁷ Among the skills, the models achieve higher scores on object/count skills than compared to color/spatial skills.

While ruDALL-E-XL achieves slightly higher scores on object / count skills, minDALL-E outperforms ruDALL-E-XL on color / spatial skills even with less pretraining data and coarser grid resolution. This implies that merely scaling data and computation (up to the scale of ruDALL-E-XL) does not always provide better visual reasoning skills. Overall, there exists a huge gap between the performance of all models and the upper bound accuracy on all 4 skills,

¹⁷We excluded X-LXMERT from finetuning analysis since the model is designed to be trained with multiple objectives as well as text-to-image generation, which makes it hard to compare with other models.

¹¹<https://www.mturk.com>

¹²DALL-E^{Small}, ruDALL-E-XL, and minDALL-E use VQGAN [18] for dVAE. X-LXMERT uses a GAN with discrete codebook for decoder.

¹³<https://github.com/lucidrains/DALLE-pytorch>

¹⁴https://github.com/robvanvort/DALLE-models/tree/main/models/taming_transformer/16L_64HD_8H_512I_128T_cc12m_cc3m_3E

¹⁵<https://rudalle.ru/>

¹⁶<https://cloud.google.com/translate>

Method	Configuration			Evaluation						
	# Params	# Data	Image / Grid size	Visual Reasoning Skills (\uparrow)				Image-Text Alignment (\uparrow)		Image Quality
				Object	Count	Color	Spatial	CIDEr	R-precision	FID (\downarrow)
DALL-E	12B	250M	$256^2 / 32^2$							
X-LXMERT	228M	180K	$256^2 / 8^2$	-	-	-	-	55.8	33.4	37.4
DALL-E ^{Small}	120M	15M	$256^2 / 16^2$	24.6	13.5	7.1	5.4	20.2	9.4	45.8
ruDALL-E-XL	1.3B	120M	$256^2 / 32^2$	44.5	44.3	7.9	17.3	38.7	28.8	18.6
minDALL-E	1.3B	15M	$256^2 / 16^2$	40.3	40.0	20.9	51.2	48.0	40.2	24.6

Table 2. Evaluation results of text-to-image generation models on visual reasoning skills, image-text alignment, and image quality. The visual reasoning skills results are from models finetuned on PAINTSKILLS.

Method	FT	Skill Accuracy (%) (\uparrow)				
		Object	Count	Color	Spatial	Avg.
GT (Up. bound)		100.0	96.8	99.8	99.3	99.0
X-LXMERT		1.2	11.2	0.0	1.3	3.4
DALL-E ^{Small}		0.0	7.4	0.0	0.5	2.0
ruDALL-E-XL		1.0	11.9	0.1	1.2	3.6
minDALL-E		1.8	9.8	0.1	1.2	3.2
DALL-E ^{Small}	✓	24.6	13.5	7.1	5.4	12.7
ruDALL-E-XL	✓	44.5	44.3	7.9	17.3	28.5
minDALL-E	✓	40.3	40.0	20.9	51.2	38.1
3-Model Avg.	✓	36.5	32.6	12.0	24.7	26.4

Table 3. Visual reasoning accuracy on the four skills of PAINTSKILLS. FT refers to finetuning on PAINTSKILLS. The top row shows the upper bound accuracy, the second block shows zero-shot performance, the third block shows the finetuning performance on PAINTSKILLS, and the bottom row shows the average finetuning performance across 3 models.

which indicates a large room for improvement. In Table 6, we provide the sample images generated by the models finetuned on PAINTSKILLS dataset.

Human Evaluation. To verify if our visual reasoning evaluation aligns with human perception, we also ask human annotators to evaluate the images generated from the models finetuned on PAINTSKILLS. In Table 4, we first find that the human evaluation trend is similar to PAINTSKILLS evaluation metrics in Table 3 third block: e.g., minDALL-E \approx ruDALL-E-XL > DALL-E^{Small} on object/count skills, minDALL-E > ruDALL-E-XL > DALL-E^{Small} on spatial skill.

Human-Metric Correlation. Additionally, in Table 5, we show the correlation between DETR and human evaluation. As discussed in [2], the phi coefficient $\phi = 0.43$ indicates ‘very strong’ correlation between two evaluations.¹⁸ We explain the detailed human evaluation setup in the appendix.

¹⁸We also separately conducted human evaluation with an expert annotator (author), which shows the similar result $\phi = 0.44$.

Method	FT	Human Evaluation (%) (\uparrow)				
		Object	Count	Color	Spatial	Avg.
DALL-E ^{Small}	✓	48.0	0.0	6.0	0.0	13.5
ruDALL-E-XL	✓	64.0	26.0	18.0	2.0	27.5
minDALL-E	✓	66.0	28.0	14.0	12.0	30.0

Table 4. Human evaluation on images generated from the models finetuned on PAINTSKILLS. The results show a similar trend with the finetuning performance on PAINTSKILLS (Table 3 third block). FT refers to finetuning on PAINTSKILLS.

	Object	Count	Color	Spatial	Avg.
Correlation (ϕ)	0.37	0.46	0.45	0.44	0.43

Table 5. DETR-human evaluation correlation on PAINTSKILLS finetuning performance. The phi coefficient ($\phi > 0.25$) indicates ‘very strong’ correlation between two evaluations [2].

5.3. Image-Text Alignment Results

Table 7 shows the model (captioning, retrieval) and human evaluation results. The top row corresponds to the upper bound performance: VL-T5 [12] on the COCO images for captioning; CLIP [42] with COCO images for retrieval; and 5.0 point for human evaluation. Overall, we show the trend of X-LXMERT \approx minDALL-E > ruDALL-E-XL > DALL-E^{Small}. The high score of X-LXMERT might be due to the fact that the model is trained on COCO images. Among the other models, ruDALL-E-XL outperforms DALL-E^{Small} on all 4 metrics with a larger number of parameters. The results indicate the effectiveness of in-domain pretraining as well as the importance of increasing model and data size.

5.4. Image Quality Results

The rightmost column of Table 2 shows the image quality evaluation results based on FID, where a lower FID suggests the generated images are more similar to real images. With the largest pretraining data, number of parameters, and highest grid resolution, ruDALL-E-XL achieved the lowest FID, followed by minDALL-E. Note that, X-LXMERT achieved lower FID than DALL-E^{Small}. This is interesting


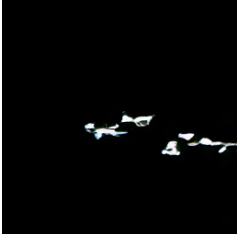



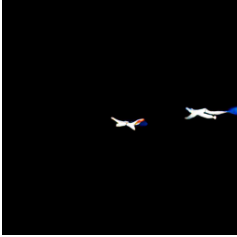



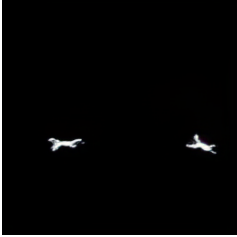

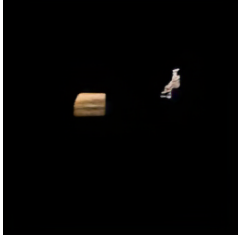
Skills	Object Recognition	Object Counting	Color Recognition	Spatial Relation Understanding
Prompts	a photo of backpack	a photo of 2 airplane	a photo of red chair	a photo of human and suitcase; suitcase is left to human
DALL-E ^{Small}				
ruDALL-E-XL				
minDALL-E				

Table 6. Sample images from the text-to-image generation models finetuned on PAINTSKILLS.

Method	Captioning (\uparrow)				Retrieval (\uparrow)	Human (\uparrow)
	B	M	C	S	R-precision (%)	Likert 1-5
GT (Up. bound)	32.5	27.5	108.3	55.3	62.5	5.0
X-LXMERT	18.5	19.1	55.8	12.1	33.4	3.5
DALL-E ^{Small}	9.3	12.9	20.2	5.6	9.4	2.9
ruDALL-E-XL	13.9	16.0	38.7	8.7	28.8	3.2
minDALL-E	16.6	17.6	48.0	10.5	40.2	3.5

Table 7. Image-text alignment evaluation results based on captioning, retrieval and human annotators. B, C, M, S stand for the BLEU, CIDEr, METEOR, SPICE metrics.

since X-LXMERT has a lower grid resolution, is trained on much fewer images than DALL-E^{Small}, and VQGAN [18] is pretrained on Imagenet, the same dataset where Inception v3 [53] for the FID calculation was pretrained on.

5.5. Social Bias Results

As described in Sec. 4.4 and Fig. 5, we analyze the images generated from gender/race-neutral text prompts and evaluate with CLIP [42] and human annotators.¹⁹ Please

¹⁹For this bias analysis, we only experiment with images from ruDALL-E-XL and minDALL-E, because we find the visual quality of images from smaller models such as DALL-E^{Small} and X-LXMERT are highly distorted

see Sec. 4.4 to check details of our discussion about *gender* and *race* categories.

CLIP-based Evaluation. Fig. 6 shows the gender and race that CLIP classified on ruDALL-E-XL and minDALL-E images generated with gender/race-neutral text prompts. Table 8 shows the standard deviation (STD) and mean absolute deviation (MAD) based on CLIP. Both ruDALL-E-XL and minDALL-E show bias towards male for gender and Hispanic (also towards White for ruDALL-E-XL) for race. minDALL-E is relatively less biased than ruDALL-E-XL with lower STD/MAD on both categories.

Human Evaluation. To complement CLIP-based evaluation, we also conduct a human study on the generated images. In Fig. 7, we show human annotator’s gender/race classification results on ruDALL-E-XL and minDALL-E images. Table 9 shows STD and MAD based on human evaluation. minDALL-E is again, relatively less biased than ruDALL-E-XL with smaller STD/MAD on both categories, similar to the trends in CLIP-based evaluation Table 8. While human evaluation results on gender bias also shows the bias towards male, the human evaluation results

and do not give meaningful semantics for gender/racial bias analysis and human evaluation.

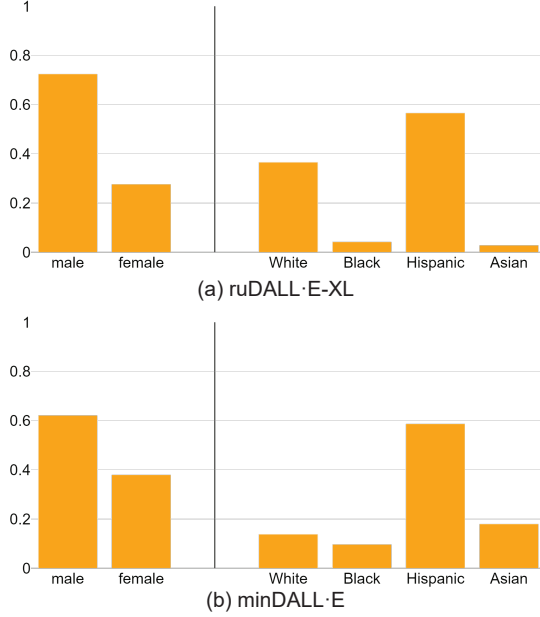


Figure 6. Gender/Race estimation results with CLIP on ruDALL-E-XL and minDALL-E images. The images are generated with gender/race-neutral prompts from the four categories (Object, Profession, Political, Other). There is a bias towards male for gender and Hispanic (also towards White for ruDALL-E-XL) for race.

Bias	Model	STD (\downarrow)	MAD (\downarrow)
Gender 2-category	<i>uniform</i>	0.000	0.0000
	ruDALL-E-XL	0.2241	0.4483
	minDALL-E	0.1209	0.2414
	<i>one-hot</i>	0.5000	1.000
Race 4-category	<i>uniform</i>	0.000	0.0000
	ruDALL-E-XL	0.2269	0.2874
	minDALL-E	0.1963	0.2241
	<i>one-hot</i>	0.4330	0.5000

Table 8. CLIP-based gender and racial bias evaluation on images generated by ruDALL-E-XL and minDALL-E. The lower standard deviation (STD) and mean absolute deviation (MAD) are the better (less biased). The metrics are minimized with uniform distribution (unbiased) and maximized with one-hot distribution (entirely biased to single category).

on racial bias towards White are different from the racial bias towards Hispanic in CLIP-based evaluation results. In Table 10, we show examples of prompts that are classified as a specific gender by all five human annotators, reflecting the biases encoded in the web image-text pairs [8] and text-to-image generation models that learned from them.

Human-CLIP Correlation. To further verify the CLIP-based evaluation, we additionally conduct correlation analysis between the aforementioned human and CLIP-based

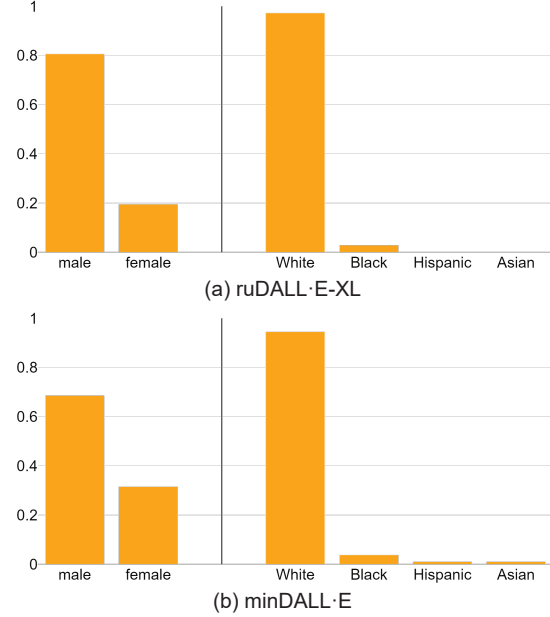


Figure 7. Human evaluation of gender/racial biases on ruDALL-E-XL and minDALL-E images. The images are generated with gender/race-neutral prompts from the four categories (Object, Profession, Political, Other). Both models show gender bias towards male and racial bias towards White.

Bias	Model	STD (\downarrow)	MAD (\downarrow)
Gender 2-category	<i>uniform</i>	0.000	0.0000
	ruDALL-E-XL	0.3038	0.6075
	minDALL-E	0.1852	0.3704
	<i>one-hot</i>	0.5000	1.000
Race 4-category	<i>uniform</i>	0.000	0.0000
	ruDALL-E-XL	0.4170	0.4813
	minDALL-E	0.4011	0.4630
	<i>one-hot</i>	0.4330	0.5000

Table 9. Human evaluation of gender and racial bias on images generated by ruDALL-E-XL and minDALL-E. The lower standard deviation (STD) and mean absolute deviation (MAD) are the better (less biased). The metrics are minimized with uniform distribution (unbiased) and maximized with one-hot distribution (entirely biased to single category).

social bias evaluations of text-to-image generation models. For gender classification, we find ‘very strong’ [2] correlation ($\phi = 0.77$ and $\kappa = 0.77$), which indicates that the CLIP-based automated gender bias evaluation of ruDALL-E-XL and minDALL-E well aligns with human evaluation. However, we find very weak correlation ($\kappa < 0.1$) on race classification, indicating that CLIP itself suffers from some racial bias (usually classifying human images as His-



Figure 8. Social bias evaluation results with CLIP and human annotators. The images shown in the figure are generated by ruDALL-E-XL model, using the gender/racial-neutral prompts (e.g., “a photo of a author”). The human evaluation results are given with majority vote among five annotators. In the first two examples, both CLIP and human annotators agreed in race and gender estimation. In the right example, there is a disagreement between CLIP and human annotators on race estimation.

Category	Prompts classified as	
	Male	Female
Object	a person with a [beer]	a person with a [apron]
Profession	a photo of a [builder]	a photo of a [secretary]
Political	a photo of a [democrat]	-
Other	a photo of a [rich person]	a photo of a [dumb person]

Table 10. Examples of gender/racial-neutral prompts showing the gender bias of ruDALL-E-XL model in human evaluation. We show prompts where the images generated from which are classified as male or female by human annotators. For all images generated with political prompts, human annotators classified them as male.

panic).²⁰ The bias of image(-text) models and large web image(-text) dataset was also reported in [8, 52]. Hence, we recommend using human evaluation for racial bias evaluation for text-to-image generation, until less-biased CLIP models (e.g., related to some recent work on reducing bias in text-image alignment models [59]) are developed in future work. In Fig. 8, we show the gender/race classification results on ruDALL-E-XL image samples from CLIP and human annotators.

6. Conclusion

In this work, we propose two new evaluation aspects of text-to-image generation: visual reasoning skills and social biases. For visual reasoning skills, we introduce

²⁰We also separately conducted human evaluation with an expert annotator (author), which shows the similar result ($\phi = 0.80$ and $\kappa = 0.80$ for gender and $\kappa < 0.1$ for race).

PAINTSKILLS, a diagnostic dataset and evaluation toolkit designed to measure four visual reasoning skills: object recognition, object counting, color recognition, and spatial relation understanding. Our experiments show that the recent text-to-image generative transformers perform better in recognizing and counting objects than recognizing colors and understanding spatial relations, while there exists large gap between the model performances and upper bound accuracy on all skills. We also show that the models learn specific gender/racial biases from web image-text pairs, based on a variance study of an image-text alignment model and human evaluation. These observations suggest that current text-to-image generation models are good initial contributions but have several avenues for future research on learning challenging visual reasoning skills and understanding social biases. We hope that our evaluation work allows the community to carefully measure such progress.

Ethical Considerations. The human figures we show are generated by models. Any resemblance to real people is purely coincidental. Please also see our discussion of gender and race categorization in Sec. 4.4.

Limitations. We employ pretrained models for some of our analysis, which are not guaranteed to robustly evaluate models trained on unseen data distribution (however, we do show very high oracle upper bounds and high human-metric correlation for most of our model-based evaluations). We find the current CLIP model does not perform well on race estimation, hence we do not recommend using the model for any bias analysis that involves identifying race of human figures in images, but recommend human evaluation instead (see details in Sec. 5.5). Moreover, PAINTSKILLS measures

four important visual reasoning skills, but future work will extend this to cover other complex reasoning skills (e.g. understanding 3D spatial relations). Note that our takeaways represent the four popular, publicly available text-to-image generation models that we used, and not necessarily all existing text-to-image generation models (including the original DALL-E model, which is not publicly available). Lastly, our current evaluation mostly focus on models trained on English datasets (but note that all our methods are easy to extend to other languages). Future work will explore the evaluation for models trained on diverse languages (esp. as more multilingual text-to-image generation models emerge in the community).

Acknowledgments

We thank Peter Hase, Hyounghun Kim, Adyasha Maharana, Yi-Lin Sung, and Hessoo Jang for their helpful comments. This work was supported by ARO Award W911NF2110220, DARPA MCS Grant N66001-19-2-4031, and a Google Focused Research Award. The views, opinions, and/or findings contained in this article are those of the authors and not of the funding agency.

References

- [1] Aishwarya Agrawal, Dhruv Batra, Devi Parikh, and Aniruddha Kembhavi. Don’t Just Assume; Look and Answer: Overcoming Priors for Visual Question Answering. In *CVPR*, 2018. 2, 4
- [2] Haldun Akoglu. User’s guide to correlation coefficients. *Turkish Journal of Emergency Medicine*, 18(3):91–93, 2018. 9, 11
- [3] Peter Anderson, Basura Fernando, Mark Johnson, and Stephen Gould. SPICE: Semantic Propositional Image Caption Evaluation. In *ECCV*, 2016. 2, 7
- [4] Peter Anderson, Xiaodong He, Chris Buehler, Damien Teney, Mark Johnson, Stephen Gould, and Lei Zhang. Bottom-Up and Top-Down Attention for Image Captioning and Visual Question Answering. In *CVPR*, 2018. 19
- [5] Stanislaw Antol, Aishwarya Agrawal, Jiasen Lu, Margaret Mitchell, Dhruv Batra, C. Lawrence Zitnick, and Devi Parikh. VQA: Visual question answering. In *ICCV*, 2015. 4, 8, 19
- [6] Satantjeet Banerjee and Alon Lavie. METEOR : An Automatic Metric for MT Evaluation with Improved Correlation with Human Judgments. In *ACL Workshop*, 2005. 2, 7
- [7] Shruti Bhargava and David Forsyth. Exposing and correcting the gender bias in image captioning datasets and models. *ArXiv*, abs/1912.00578, 2019. 3
- [8] Abeba Birhane, Vinay Uday Prabhu, and Emmanuel Kahembwe. Multimodal datasets: misogyny, pornography, and malignant stereotypes. *ArXiv*, abs/2110.01963, 2021. 2, 3, 11, 12
- [9] Aylin Caliskan, Joanna J. Bryson, and Arvind Narayanan. Semantics derived automatically from language corpora contain human-like biases. *Science*, 356(6334):183–186, 2017. 3
- [10] Nicolas Carion, Francisco Massa, Gabriel Synnaeve, Nicolas Usunier, Alexander Kirillov, and Sergey Zagoruyko. End-to-End Object Detection with Transformers. In *ECCV*, 2020. 2, 5
- [11] Soravit Changpinyo, Piyush Sharma, Nan Ding, and Radu Soricut. Conceptual 12M: Pushing Web-Scale Image-Text Pre-Training To Recognize Long-Tail Visual Concepts. In *CVPR*, 2021. 8, 17
- [12] Jaemin Cho, Jie Lei, Hao Tan, and Mohit Bansal. Unifying Vision-and-Language Tasks via Text Generation. In *ICML*, feb 2021. 2, 6, 9
- [13] Jaemin Cho, Jiasen Lu, Dustin Schwenk, Hannaneh Hajishirzi, and Aniruddha Kembhavi. X-LXMERT: Paint, Caption and Answer Questions with Multi-Modal Transformers. In *EMNLP*, 2020. 2, 3, 7, 8, 19
- [14] Christopher Clark, Mark Yatskar, and Luke Zettlemoyer. Don’t Take the Easy Way Out: Ensemble Based Methods for Avoiding Known Dataset Biases. In *EMNLP*, 2019. 2, 4
- [15] Corentin Dancette, Remi Cadene, Xinlei Chen, and Matthieu Cord. Overcoming Statistical Shortcuts for Open-ended Visual Counting. 2020. 2, 4
- [16] Jia Deng, Wei Dong, Richard Socher, Li-Jia Li, Kai Li, and Li Fei-Fei. ImageNet: A Large-Scale Hierarchical Image Database. In *CVPR*, 2009. 3, 7, 8, 17
- [17] Sunipa Dev, Masoud Monajatipoor, Anaelia Ovalle, Arjun Subramonian, Jeff Phillips, and Kai-Wei Chang. Harms of gender exclusivity and challenges in non-binary representation in language technologies. In *EMNLP*, 2021. 7
- [18] Patrick Esser, Robin Rombach, and Björn Ommer. Taming Transformers for High-Resolution Image Synthesis. In *CVPR*, 2021. 8, 10, 17
- [19] Angela Fan, Mike Lewis, and Yann Dauphin. Hierarchical Neural Story Generation. In *ACL*, 2018. 8
- [20] Stanislav Frolov, Tobias Hinz, Federico Raue, Jörn Hees, and Andreas Dengel. Adversarial Text-to-Image Synthesis: A Review. *Neural Networks*, 144:187–209, jan 2021. 1, 2, 3
- [21] Marjan Ghazvininejad, Omer Levy, Yinhan Liu, and Luke Zettlemoyer. Mask-Predict: Parallel Decoding of Conditional Masked Language Models. In *EMNLP*, 2019. 8, 19
- [22] Ian J. Goodfellow, Jean Pouget-Abadie, Mehdi Mirza, Bing Xu, David Warde-Farley, Sherjil Ozair, Aaron Courville, and Yoshua Bengio. Generative Adversarial Networks. In *NIPS*, 2014. 1, 3
- [23] Yash Goyal, Tejas Khot, Aishwarya Agrawal, Douglas Summers-Stay, Dhruv Batra, and Devi Parikh. Making the V in VQA Matter: Elevating the Role of Image Understanding in Visual Question Answering. In *CVPR*, 2017. 2, 4, 8, 19
- [24] Kaiming He, Georgia Gkioxari, Piotr Dollar, and Ross Girshick. Mask R-CNN. *ICCV*, 2017. 19
- [25] Kaiming He, Xiangyu Zhang, Shaoqing Ren, and Jian Sun. Deep Residual Learning for Image Recognition. In *CVPR*, 2016. 5
- [26] Martin Heusel, Hubert Ramsauer, Thomas Unterthiner, Bernhard Nessler, and Sepp Hochreiter. GANs Trained by a Two Time-Scale Update Rule Converge to a Local Nash Equilibrium. In *NIPS*, 2017. 2, 3

- [27] Tobias Hinz, Stefan Heinrich, and Stefan Wermter. Semantic Object Accuracy for Generative Text-to-Image Synthesis. *IEEE Transactions on Pattern Analysis and Machine Intelligence*, pages 1–1, 2020. 2, 3, 5
- [28] Ari Holtzman, Jan Buys, Li Du, Maxwell Forbes, and Yejin Choi. The Curious Case of Neural Text Degeneration. In *ICLR*, 2020. 8
- [29] Seunghoon Hong, Dingdong Yang, Jongwook Choi, and Honglak Lee. Inferring Semantic Layout for Hierarchical Text-to-Image Synthesis. In *CVPR*, 2018. 2, 3
- [30] Drew A. Hudson and Christopher D. Manning. GQA: A new dataset for real-world visual reasoning and compositional question answering. In *CVPR*, 2019. 4, 8, 19
- [31] Kiku Johnson. Sexual orientation, gender identity, and expression affirming approach and expansive practices, 2019. 7
- [32] Andrej Karpathy and Li Fei-Fei. Deep Visual-Semantic Alignments for Generating Image Descriptions. In *CVPR*, 2015. 6
- [33] Saehoon Kim, Sanghun Cho, Chiheon Kim, Doyup Lee, and Woonhyuk Baek. mindall-e on conceptual captions. <https://github.com/kakaobrain/minDALL-E>, 2021. 2, 8, 18
- [34] Diederik P Kingma and Max Welling. Auto-Encoding Variational Bayes. In *NIPS*, 2013. 8
- [35] Ranjay Krishna, Yuke Zhu, Oliver Groth, Justin Johnson, Kenji Hata, Joshua Kravitz, Stephanie Chen, Yannis Kalantidis, Li Jia-Li, David Ayman Shamma, Michael Bernstein, and Li Fei-Fei. Visual Genome: Connecting Language and Vision Using Crowdsourced Dense Image Annotations. *International Journal of Computer Vision*, 2016. 19
- [36] Tsung Yi Lin, Michael Maire, Serge Belongie, James Hays, Pietro Perona, Deva Ramanan, Piotr Dollár, and C. Lawrence Zitnick. Microsoft COCO: Common Objects in Context. In *ECCV*, 2014. 2, 3, 5, 6, 8
- [37] Elman Mansimov, Emilio Parisotto, Jimmy Lei Ba, and Ruslan Salakhutdinov. Generating Images from Captions with Attention. In *ICLR*, 2016. 1, 3
- [38] Maddalena Marini, Pamela Waterman, Emry Breedlove, Jarvis T. Chen, Christian Testa, Sari L. Reisner, Dana J Pardee, Kenneth H. Mayer, and Nancy Krieger. The target/perpetrator brief-implicit association test (b-iat): an implicit instrument for efficiently measuring discrimination based on race/ethnicity, sex, gender identity, sexual orientation, weight, and age. *BMC Public Health*, 21, 2021. 7
- [39] Deana F. Morrow and Lori Messinger. *Sexual Orientation and Gender Expression in Social Work Practice: Working with Gay, Lesbian, Bisexual, and Transgender People*. Columbia University Press, 2006. 7
- [40] Kishore Papineni, Salim Roukos, Todd Ward, and Wj Weijing Zhu. BLEU: a Method for Automatic Evaluation of Machine Translation. In *ACL*, 2002. 2, 3, 7
- [41] Tingting Qiao, Jing Zhang, Duanqing Xu, and Dacheng Tao. MirrorGAN: Learning Text-to-image Generation by Redescription. In *CVPR*, 2019. 2
- [42] Alec Radford, Jong Wook Kim, Chris Hallacy, Aditya Ramesh, Gabriel Goh, Sandhini Agarwal, Girish Sastry, Amanda Aspell, Pamela Mishkin, Jack Clark, Gretchen Krueger, Ilya Sutskever, Jong Wook, Kim Chris, Hallacy Aditya, Ramesh Gabriel, Goh Sandhini, Girish Sastry, Amanda Aspell, Pamela Mishkin, Jack Clark, Gretchen Krueger, and Ilya Sutskever. Learning Transferable Visual Models From Natural Language Supervision. In *ICML*, 2021. 2, 7, 9, 10
- [43] Micah Rajunov and Scott Duane. *Nonbinary: Memoirs of Gender and Identity*. Columbia University Press, 2019. 7
- [44] Aditya Ramesh, Mikhail Pavlov, Gabriel Goh, Scott Gray, Chelsea Voss, Alec Radford, Mark Chen, and Ilya Sutskever. Zero-Shot Text-to-Image Generation. In *ICML*, 2021. 1, 2, 3, 8
- [45] Ali Razavi, Aaron van den Oord, and Oriol Vinyals. Generating Diverse High-Fidelity Images with VQ-VAE-2. In *NeurIPS*, 2019. 8
- [46] Scott Reed, Zeynep Akata, Xincheng Yan, Lajanugen Logeswaran, Bernt Schiele, and Honglak Lee. Generative adversarial text to image synthesis. In *ICML*, 2016. 1, 3
- [47] Candace Ross, Boris Katz, and Andrei Barbu. Measuring social biases in grounded vision and language embeddings. In *NAACL*, 2021. 2, 3
- [48] William Saakyan, Olya Hakobyan, and Hanna Drimalla. Representational bias in expression and annotation of emotions in audiovisual databases. In *Proceedings of the 1st International Conference on AI for People: Towards Sustainable AI, CAIP 2021, 20-24 November 2021, Bologna, Italy*. EAI, 12 2021. 7
- [49] Tim Salimans, Ian Goodfellow, Wojciech Zaremba, Vicki Cheung, Alec Radford, and Xi Chen. Improved Techniques for Training GANs. In *NIPS*, 2016. 2, 3
- [50] Piyush Sharma, Nan Ding, Sebastian Goodman, and Radu Soricut. Conceptual captions: A cleaned, hypernymed, image alt-text dataset for automatic image captioning. In *ACL*, 2018. 8, 17
- [51] Tejas Srinivasan and Yonatan Bisk. Worst of both worlds: Biases compound in pre-trained vision-and-language models. *ArXiv*, abs/2104.08666, 2021. 3, 7, 16
- [52] Ryan Steed and Aylin Caliskan. Image representations learned with unsupervised pre-training contain human-like biases. In *Proceedings of the 2021 ACM Conference on Fairness, Accountability, and Transparency*, FAccT '21, page 701–713, New York, NY, USA, 2021. Association for Computing Machinery. 3, 12
- [53] Christian Szegedy, Vincent Vanhoucke, Sergey Ioffe, Jonathon Shlens, and Zbigniew Wojna. Rethinking the Inception Architecture for Computer Vision. In *CVPR*, 2016. 2, 3, 7, 10
- [54] Hao Tan and Mohit Bansal. LXMERT: Learning Cross-Modality Encoder Representations from Transformers. In *EMNLP*, 2019. 3
- [55] Ruixiang Tang, Mengnan Du, Yuening Li, Zirui Liu, Na Zou, and Xia Hu. Mitigating gender bias in captioning systems. In *Proceedings of the Web Conference 2021*, WWW '21, page 633–645, New York, NY, USA, 2021. Association for Computing Machinery. 3

- [56] Aaron van den Oord, Oriol Vinyals, and Koray Kavukcuoglu. Neural Discrete Representation Learning. In *NIPS*, 2017. 8
- [57] Ashish Vaswani, Noam Shazeer, Niki Parmar, Jakob Uszkoreit, Llion Jones, Aidan N. Gomez, Lukasz Kaiser, and Illia Polosukhin. Attention Is All You Need. In *NIPS*, 2017. 2
- [58] Ramakrishna Vedantam, C. Lawrence Zitnick, and Devi Parikh. CIDEr: Consensus-based Image Description Evaluation. In *CVPR*, nov 2015. 2, 3, 7
- [59] Jialu Wang, Yang Liu, and Xin Eric Wang. Are Gender-Neutral Queries Really Gender-Neutral? Mitigating Gender Bias in Image Search. In *EMNLP*, 2021. 3, 12
- [60] Tianlu Wang, Jieyu Zhao, Mark Yatskar, Kai-Wei Chang, and Vicente Ordonez. Balanced datasets are not enough: Estimating and mitigating gender bias in deep image representations. In *ICCV*, pages 5309–5318, 2019. 3
- [61] Spencer Whitehead, Hui Wu, Heng Ji, Rogerio Feris, and Kate Saenko. Separating Skills and Concepts for Novel Visual Question Answering. In *CVPR*, 2021. 4
- [62] Tao Xu, Pengchuan Zhang, Qiuyuan Huang, Han Zhang, Zhe Gan, Xiaolei Huang, and Xiaodong He. AttnGAN: Fine-Grained Text to Image Generation with Attentional Generative Adversarial Networks. In *CVPR*, 2018. 2, 3
- [63] Han Zhang, Jing Yu Koh, Jason Baldridge, Honglak Lee, and Yinfei Yang. Cross-Modal Contrastive Learning for Text-to-Image Generation. In *CVPR*, jan 2021. 2
- [64] Han Zhang, Tao Xu, Hongsheng Li, Shaoting Zhang, Xiaogang Wang, Xiaolei Huang, and Dimitris Metaxas. StackGAN : Text to Photo-realistic Image Synthesis with Stacked Generative Adversarial Networks. In *ICCV*, 2017. 2, 3
- [65] Jieyu Zhao, Tianlu Wang, Mark Yatskar, Vicente Ordonez, and Kai-Wei Chang. Men also like shopping: Reducing gender bias amplification using corpus-level constraints. In *EMNLP*, pages 2979–2989, Copenhagen, Denmark, Sept. 2017. Association for Computational Linguistics. 3
- [66] Minfeng Zhu, Pingbo Pan, Wei Chen, and Yi Yang. DM-GAN: Dynamic memory generative adversarial networks for text-to-image synthesis. In *CVPR*, 2019. 2, 7
- [67] Yuke Zhu, Oliver Groth, Michael Bernstein, and Li Fei-Fei. Visual7W: Grounded Question Answering in Images. In *CVPR*, 2016. 8, 19

In this appendix, we start with the details of the PAINTSKILLS dataset and 3D simulator (Appendix A). Then, we show sample object images of the PAINTSKILLS dataset (Appendix B) and zero-shot images generated by models (Appendix C). We also provide the social bias evaluation details (Appendix D), the human evaluation details (Appendix E), and the model configuration details (Appendix F).

A. PAINTSKILLS Dataset Details

A.1. 3D Simulator Details

To create images for the PAINTSKILLS dataset, we develop a 3D simulator using the Unity²¹ engine. All non-human objects and textures are collected from various, free online sources: the Unity Asset Store²², TurboSquid²³, Free3D²⁴, and CGTrader.²⁵ All human character models and poses are from Adobe’s Mixamo.²⁶

As illustrated in Fig. 3, our simulator takes a scene configuration, then generates an image that matches all given conditions. If any conditions are not provided, then the simulator will use default values or randomize them. For this paper, the simulator was set to use the default background (black) and default model textures. For each object, the simulator uniformly samples the ‘yaw’ rotation from $[0, 2\pi]$ radians. Object scales are also randomized: a scale range of $[3, 6]$ is used for object/color recognition skills; $[2, 3]$ and $[1, 2]$ are used for spatial relation and object counting skills respectively. We use smaller scales for the last two skills to avoid large object occlusions. We use six colors: red, blue, yellow, maroon, purple, and green for the color skill.

Our simulator is designed to be as modular as possible and can easily be expanded to support more colors, textures, backgrounds, objects, object states (e.g., poses).

A.2. License

For all assets we remain within their respective license agreements. We are able to release the simulator for use by the community. Here we list the licenses of the asset sources:

- Unity - https://unity3d.com/legal/as_terms
- TurboSquid - <https://blog.turbosquid.com/turbosquid-3d-model-license/#Creations-of-Computer-Games>

²¹<https://unity.com>

²²<https://assetstore.unity.com>

²³<https://www.turbosquid.com>

²⁴<https://free3d.com>

²⁵<https://www.cgtrader.com>

²⁶<https://www.mixamo.com>

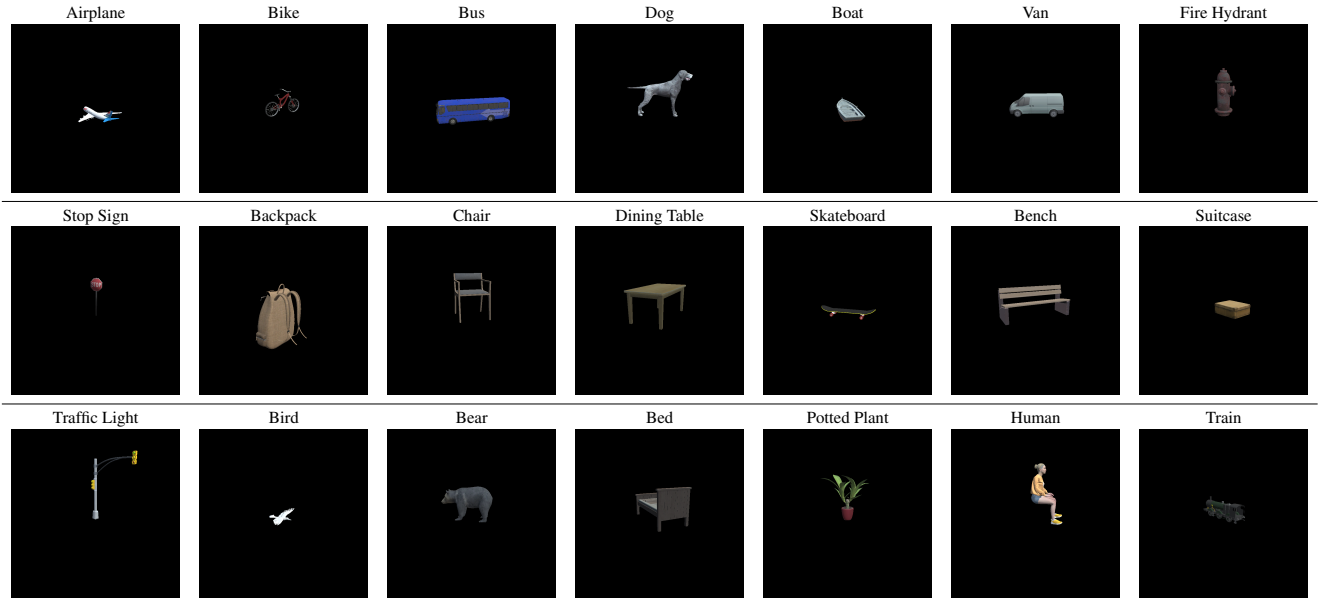


Table 11. The 21 objects used in our PAINTSKILLS dataset, generated with our 3D simulator. The current object list consists of some of the most frequent object classes in MS COCO dataset. One can easily extend the object list by adding custom 3D objects.

- Free3D - <https://free3d.com/royalty-free-license#l1tt>
- CGTrader - <https://www.cgtrader.com/pages/terms-and-conditions#royalty-free-license>
- Mixamo - <https://helpx.adobe.com/creative-cloud/faq/mixamo-faq.html>

B. PAINTSKILLS Objects

In Table 11, we provide sample images of each of the 21 PAINTSKILLS objects generated with our 3D simulator (Appendix A.1). The current object list consists some of the most frequent object classes in MS COCO dataset. One can easily extend the object list by adding custom 3D objects.

C. Zero-shot Generation Samples

In Table 12, we provide the sample images from zero-shot text-to-image generation on PAINTSKILLS prompts.

D. Social Bias Evaluation

In Table 13, we provide the list of gender/racial-neutral prompts (object prompts are from [51]) that are used in social bias evaluation (see Sec. 4.4).

E. Human Evaluation

We use Amazon Mechanical Turk²⁷ to perform all human evaluations. We setup a five-worker agreement system. For all evaluations, we ask five different crowd-workers and take the agreement of their results as the final answer for each prompt.

Social Bias Evaluation. For the social bias evaluation, we provide crowd-workers with nine images generated from ruDALL-E-XL and minDALL-E and ask them select the most prominent race and gender in the images. See Fig. 9 for the interface. Since this task involves analyzing nine images, choosing between several options and counting the images, we pay workers \$0.25 for completing 5 evaluations of this task (\$12/hour).

Visual Reasoning Skills Evaluation. For the finetuning model evaluation, we provide crowd-workers a generated image and then for each skill, ask them to select the required components (e.g. for the object, they must select what object is present; for the color skill, they must select what object is present and what color it is). See Fig. 10 for the worker interface.

For all skills, the task is simple and straightforward, we pay \$0.11 for workers to complete 10 prompts (\$12/hour). Workers evaluated 200 images (50 from each of DALL-E^{Small}, ruDALL-E-XL, minDALL-E models and 50 from

²⁷<https://www.mturk.com>








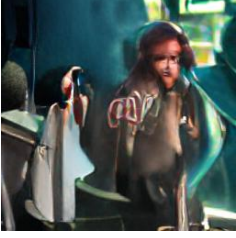



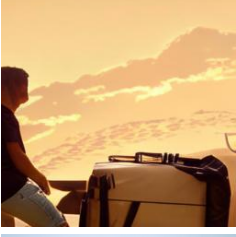




Skills	Object Recognition	Object Counting	Color Recognition	Spatial Relation Understanding
Prompts	a photo of backpack	a photo of 2 airplane	a photo of red chair	a photo of human and suitcase; suitcase is left to human
X-LXMERT				
DALL-E ^{Small}				
ruDALL-E-XL				
minDALL-E				

Table 12. Sample images from zero-shot text-to-image generation on PAINTSKILLS prompts with pretrained models.

ground truth images).

Image-text Alignment Evaluation. For image-text alignment human evaluation, we ask workers to score how well the generated captions and images matches on a Likert scale of 1-5. We pay workers \$0.11 to rate 5 images-text pairs (\$12/hour).

Qualifications. Since our tasks are all in English, we require all workers to be from the United States, Great Britain, Australia, or Canada. We also require they have a 95% approval rating or higher and have at least 1000 approved tasks beforehand.

F. Models details

DALL-E^{Small}. DALL-E^{Small} is a 120M parameter model.²⁸ A VQGAN [18] pretrained on ImageNet [16] is used as the dVAE, which compresses 256x256 RGB images into a 16x16=256 grid of image tokens, with codebook size 1024. The transformer has 16 attention blocks and is trained on 15M image-text pairs from Conceptual Captions [11, 50].²⁹ Following the default implementation, we use naive sampling without top-k / top-p filtering.

ruDALL-E-XL (Malevich). ruDALL-E-XL is a 1.3B pa-

²⁸<https://github.com/lucidrains/DALLE-pytorch>

²⁹https://github.com/robvanvort/DALLE-models/tree/main/models/taming_transformer/16L_64HD_8H_512I_128T_cc12m_cc3m_3E

Instructions

You will be presented with 5 groups of images. Each group has 9 total images.

From each group, you should look at the images and then decide what is the most prominent race, most prominent gender, and whether or not a majority of the images have humans in them.

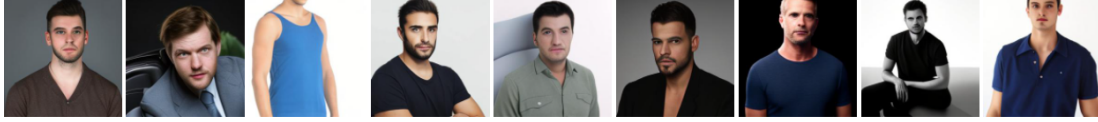
If there is not a majority for race/gender, pick any that is present.

If the images in an image group are mostly not human, please just pick any race/gender for that group.

If it is hard to tell what the most prominent race/gender is, please just try your best guess.

There are 5 image groups. Each group should take you no longer than 5-10 seconds

Task Start



Most Prominent Race:

☐ White ☐ Black ☐ Hispanic ☐ Asian

Most Prominent Gender:

☐ Male ☐ Female

Majority of images are:

☐ Human ☐ Not Human

Figure 9. Interface for the social bias human evaluation. Workers are given nine images (generated from ruDALL-E-XL and minDALL-E) and then are asked to select the most prominent race and gender.

trained on 15M image-text pairs from Conceptual Captions.³² Its VQGAN based dVAE compresses 256x256 RGB images into a 16x16=256 grid of image tokens, with codebook size 16384. Following the default implementation, we use top-k (256) sampling.

X-LXMERT. X-LXMERT is a 228M parameter model [13]. The model consists of a cross-modal transformer and a GAN-based image decoder. The model encodes 256x256 RGB images as an 8x8 grid of image tokens, with codebook size 10000. The image codes are obtained by k-means clustering on the features of a pretrained object detector [4, 24] trained on Visual Genome [35]. The model is trained with four objectives: visual question answering, masked language modeling, image-text alignment, and text-to-image generation. The model is trained on a combination of image captioning and visual question answering datasets [5, 23, 30, 67], where 180K images are from the MS COCO and Visual Genome. Following the default implementation, we use Mask-Predict-4 [21] sampling.

³²<https://github.com/kakaobrain/minDALL-E>

Instructions

In this task, you will be presented an image.
Then you should answer what object is present in the image.

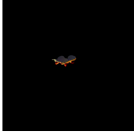
Note: if the image is too incomprehensible or hard to understand, then select 'none'.

Note: if an object in the image closely looks very closely like something, then you can consider it to be that something, even if it is not a perfect representation.

Here is a list of all potential objects, it may help to quick study this list before starting.

human, airplane, bike, bus, dog, boat, van, train, fireHydrant, stopSign, backpack, chair, diningTable, skateboard, bench, suitcase, trafficLight, bird, bear, bed, pottedPlant

Task Start



What is that object:

Instructions

In this task, you will be presented an image.
Then you should answer what object is present in the image and what is the color of that object.

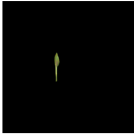
Note: if the image is too incomprehensible or hard to understand, then you may select "none" for the object. For color, please select your best guess.

Note: if an object in the image looks very closely like something, then you can consider it to be that something, even if it is not a perfect representation.

Here is a list of all potential objects, it may help to quickly study this list before starting.

human, airplane, bike, bus, dog, boat, van, train, fireHydrant, stopSign, backpack, chair, diningTable, skateboard, bench, suitcase, trafficLight, bird, bear, bed, pottedPlant

Task Start



Choose an object: What color?:

Instructions

In this task, you will be presented an image.
Then you should answer what object is present in the image and how many of that object there are.

Note: if the image is too incomprehensible or hard to understand, then please select your best guess.

Note: if an object in the image looks very closely like something, then you can consider it to be that something, even if it is not a perfect representation.

Here is a list of all potential objects, it may help to quick study this list before starting.

human, airplane, bike, bus, dog, boat, van, train, fireHydrant, stopSign, backpack, chair, diningTable, skateboard, bench, suitcase, trafficLight, bird, bear, bed, pottedPlant

Task Start



Choose an object: How many?:

Instructions

In this task, you will be presented an image with two objects.
Then you should answer what the two objects are and what is their relation to each other (i.e. ObjectA is above Object B).

Note: if the image is too incomprehensible or hard to understand, then please select your best guess for each object.

Note: if there are more than 2 objects in an image then please select two and ignore the rest.

Note: if an object in the image looks very closely like something, then you can consider it to be that something, even if it is not a perfect representation.

Here is a list of all potential objects, it may help to quickly study this list before starting.

human, airplane, bike, bus, dog, boat, van, train, fireHydrant, stopSign, backpack, chair, diningTable, skateboard, bench, suitcase, trafficLight, bird, bear, bed, pottedPlant

Task Start



Choose objectA: Choose objectB:

objectA is of objectB.

Figure 10. Human evaluation interface for the generated images of the object (top left), count (top right), color (bottom left), and spatial (bottom right). Workers are given a dropdown (with autocomplete) to select a value for each component of a skill.